Mathematical & Computational Applications, Vol. 9, No. 1, pp. 25-39, 2004

NUMERICAL SIMULATIONS OF FLOW DISTRIBUTION IN UNPACKED AND PARTIALLY PACKED VESSELS

Habib D. Zughbi and Saiffudin Sheikh
Department of Chemical Engineering
King Fahd University of Petroleum & Minerals,
Dhahran 31261, Saudi Arabia
hdzughbi@kfupm.edu.sa

Abstract- In this study, flow in an unpacked and a partially packed vessels is investigated using numerical simulations. The effects of various factors including the number of inlets and outlets, and throttling the jets by inserting orifice plates above them on the flow fields are investigated. Other factors investigated include fluid flow-rate and turbulence model. It was found that for a given number and location inlets and outlets, the injection velocity does not have a very significant impact on the flow distribution. This distribution could be improved with a careful choice of the number and location of inlets and outlets. For partially packed vessels, the packing may behave like a good distributor depending on the resistance to flow offered by the bed.

Key Words- Simulation, Flow Distribution, Partially Packed Vessel

1. INTRODUCTION

Fluid flow plays a significant role in a wide range of operations in the oil, chemical and petrochemical industry. Flow related problems in the industry are numerous. Oleimans [1] and Coleman [2] have described many of these problems in details. A good understanding of flow behavior and flow distribution is often crucial for proper design and operation of equipments such as packed and unpacked reactors and mixers. However, the detailed knowledge about the flow in industrial vessels is rather limited mainly because most vessels are operated at high temperature and pressure, which makes measurements of velocities a difficult task.

In order to model the main flow features, many simplifying assumptions are usually made, such as assuming that the flow is steady, or restricted to less than three dimensions. Computational Fluid Dynamics (CFD) offers the possibility of predicting the detailed flow and turbulence of the reactor under different geometrical and operating conditions.

This study is concerned with single-phase flows. However, two-phase flows are frequently encountered. Two most common approaches to modeling gas-liquid two-phase flows are the Euler-Euler or two fluid approach and the Euler-Lagrange or discrete bubble approach. In the Euler-Euler approach, both phases are modeled as two interpenetrating continua.

The present work is concerned with the detailed understanding of flows in unpacked and partially packed vessels mainly in two-dimensions. The effects of

flowrates, number and arrangement of inlets and outlets and geometric inserts are investigated.

1.1. Flow Through Packed Beds

In one type of modelling flow in porous media, a zone is defined in which the porous media model is applied and the pressure loss in the flow is determined via user-defined inputs. Typically a porous media model incorporates an empirically determined flow resistance in a region of the model defined as porous. A porous media model is nothing more than an added momentum sink in the governing momentum equations.

In industrial packed beds, some nonuniformities either due to the presence of internal structures as suggested by Berninger and Vortmeyer [3] or due to irregular gas inlet design as suggested by Szekely and Poveromo [4], could cause the flow not to be one-dimensional and the gas velocity to vary in both radial and axial direction. In general, three types of mathematical models have been developed for the treatment of non-parallel gas flow in packed beds (Jiang *et al.* [5]). They are (i) Vectorized Ergun equation model, (ii) Equations of motion model and (iii) Discrete cell model (DCM). In this paper the second model is used and is the only one that is discussed in details.

The Equations of motion model, in principal, solves the mass and momentum conservation equations for the flowing phase provided the solid boundaries are precisely specified. By employing the effective viscosity as an adjusting factor, a mathematical model for the interstitial velocity distribution has been developed by previous workers, namely Ziolkowska and Ziolkowski [6] and Bey and Eigenberger [7].

Fluid flow between particles in packed beds is characterized by a random packing geometry, high turbulence and strong velocity fluctuations. Any realistic flow model must therefore be based on some averaging assumptions. One generally accepted procedure suggested by Bey and Eigenberger [7] is to assume a continuous distribution of the void fraction in the packing. Then any fluid flow will create continuously distributed interstitial velocity. The flow field can be described by the Navier-Stokes equations if additional terms for fluid-particle interactions are incorporated. The application of the extended Brinkman equation where the fluid-particle interactions is described by a two-dimensional Ergun pressure correlation and the fluid wall friction is separately taken into account has been proposed (Vortemeyer and Schuster [8]).

In this investigation the approach of Bey and Eigenberger [7] has been used. The details are discussed in following section. The pressure drop in the packing has been evaluated by the well-established correlation of Ergun.

2. PRESSURE DROP CORRELATIONS FOR PACKED BED

Ergun [9] has given an expression for pressure losses in packed beds which is caused by simultaneous kinetic and viscous energy losses, and derived a comprehensive equation applicable to all types of flow. Brinkman [10] was the first to formulate the differential equation which describes the artificial flow profile within a porous medium bounded by a rigid wall restricting himself to the Darcy flow regime and extending Darcy's law by a viscosity term. Vortemeyer and Schuster [8] have used the extended Brinkman's equation for their formulation for higher flow rates by incorporating the Ergun pressure loss relation given above.

Bey and Eigenberger [7] have represented the pressure drop in the packing by modifying the Ergun equation for a cylindrical coordinated system. In the Cartesian coordinate system the pressure forces can be calculated by the following equations:

$$F_z = 150\mu_f \frac{(1-\theta)^2}{\theta^3 d_p^2} v_{z,o} + 1.75\rho_f \frac{(1-\theta)}{\theta^3 d_p} v_{z,o}|v_o| \quad (1)$$

where

$$v_z = \frac{v_{z,o}}{\theta} \quad (2)$$

$$F_y = 150\mu_f \frac{(1-\theta)^2}{\theta^3 d_p^2} v_{y,o} + 1.75\rho_f \frac{(1-\theta)}{\theta^3 d_p} v_{y,o}|v_o| \quad (3)$$

where

$$v_y = \frac{v_{y,o}}{\theta} \quad (4)$$

where F_z, is the pressure force in the z-direction, F_y, is the pressure force in the y-direction, μ_f is the dynamic viscosity (kg/ms), θ, is the void fraction, ρ_f, is the fluid density (kg/m^3), v_z, is the interstitial velocity in the z-direction (m/s), v_y, is the interstitial velocity in the y-direction (m/s), v_o, is the average empty tube flow velocity ($=\sqrt{v^2_{z,o} + v^2_{y,o}}$), $v_{z,o}$, is the average empty tube flow velocity in z- direction (m/s), $v_{y,o}$, is the average empty tube flow velocity in y direction (m/s)

The values of F_z and F_y obtained from equations (1-4) can be substituted in the momentum balance equations and solved. In the present equations the modified form of Ergun equation given by Bey and Eigenberger [7] as given from equations (1-4), have been used for calculating the pressure drop in the z- and y- directions.

3. NUMERICAL MODEL

The vessel simulated in this study is a horizontal cylinder 4.9 m in diameter and 18.2 m long. A gas stream is injected into the bottom of the vessel through three inlets each of 0.6-m diameter. The vessel has a single 1.0 m diameter outlet as shown schematically in Figure 1.

A two-dimensional model is constructed of this vessel. A mesh of 182 cells in the y-direction and 49 cells in the z-direction is chosen. This implies a uniform grid of 10 cm a side. In the y-direction, the inlets are located between cells 21-26, 89-94 and cells 157-162. The outlet is located at z = 4.9 m and in the y-direction has cells 50-59 open as shown in Figure 1.

The density of the inlet gas is 1.36 kg/m^3 and its kinematic viscosity is 2.18×10^{-5} m^2/s or a dynamic viscosity of 2.96×10^{-5} Pa.s. The gas is injected into the converter at a velocity of 57 m/s. The effects of chemical reactions and heat transfer are not included and only the flow and the pressure fields are resolved.

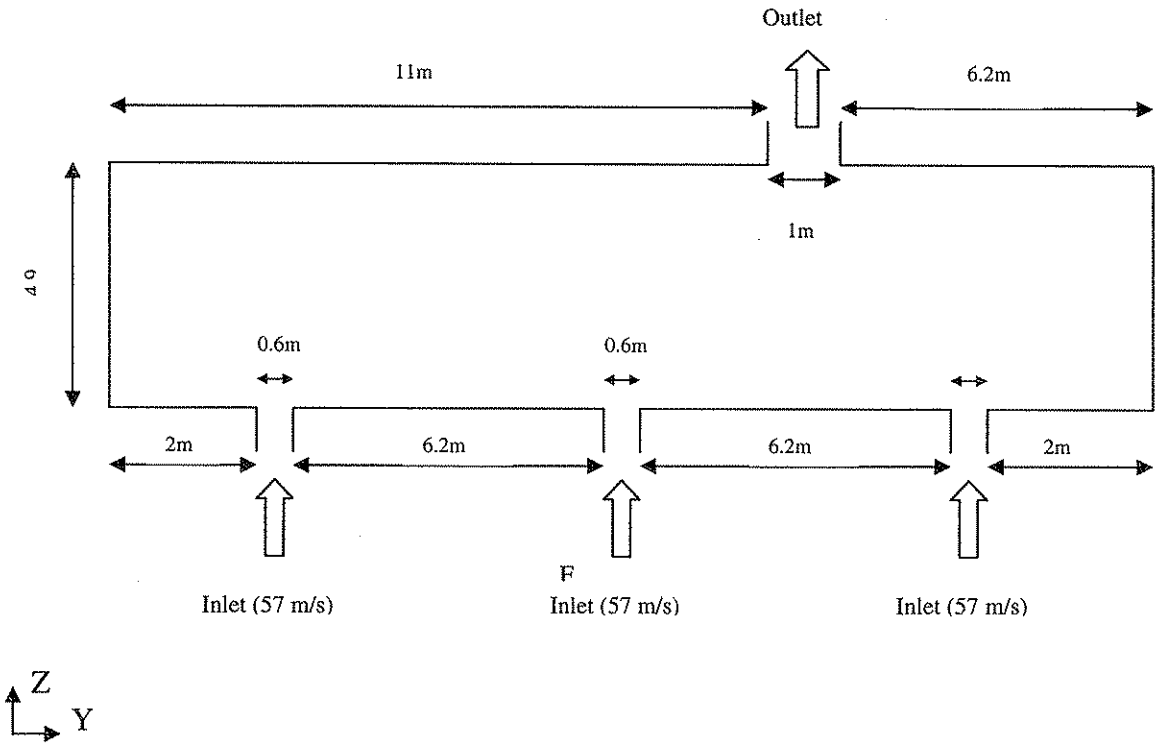

Figure 1. Schematic of the simulated vessel

The mass, momentum and energy conservation differential equations can also be written in the more general form:

$$\frac{\partial\left(R_i\rho_i\ \varphi_i\right)}{\partial t}+\mathrm{div}\left(R_i\rho_i v_i\varphi_i-R_i\Gamma_{\varphi_i}\,grad\varphi_i\right)=R_iS_{\varphi_i} \qquad (5)$$

Transient Convection Diffusion Source

where

R_i volume fraction of phase *i*

φ_i any conserved property of phase *i*

v_i velocity vector of phase *i*

Γ_{φ_i} exchange coefficient of ϕ in phase *i*

S_{φ_i} source rate of φ_i per unit volume

Thus, the Continuity equation for phase *i* becomes:

$$\frac{\partial(R_i \rho_i)}{\partial t} + \mathrm{div}(R_i \rho_i v_i) = R_i S_{\varphi_i} \qquad (6)$$

where

ρ_i is the density of phase *i*

and the Conservation of momentum for variable φ_i becomes:

$$\mathrm{div}(R_i \rho_i v_i \varphi_i - R_i \mu_{eff} \, grad \varphi_i) = R_i S_{\varphi_i} \qquad (7)$$

where

μ_{eff} is the effective viscosity

For the single-phase model the term $i = 1$ and the equations are reduced to one phase only. Gravitational body forces are represented by way of sources of momentum in the equations for each of the three velocity components for each phase. Such sources are specified in a way that ensures the multiplication of the acceleration due to gravity by the mass of the phase in the velocity cell, which results in the source being set to the force acting on the velocity cell.

The standard k-ε model is a semi-empirical model based on model transport equations for the turbulent kinetic energy (k) and its dissipation rate (ε). The model transport equation for k is derived from the exact equation, while the model transport equation for ε was obtained using physical reasoning and bears little resemblance to its mathematically exact counterpart. In the derivation of the k-ε model, it was assumed that the flow is fully turbulent, and the effects of molecular viscosity are negligible. The standard k-ε model is therefore valid only for fully turbulent flows.

The turbulent kinetic energy, k, and its rate of dissipation, ε, are obtained from the following transport equations (see PHOENICS manuals [11]):

$$\rho \frac{Dk}{Dt} = \frac{\partial}{\partial x_i}\left[\left(\mu + \frac{\mu_t}{\sigma_k}\right)\frac{\partial k}{\partial x_i}\right] + G_k + G_b - \rho\varepsilon - Y_M \qquad (8)$$

$$\rho \frac{D\varepsilon}{Dt} = \frac{\partial}{\partial x_i}\left[\left(\mu + \frac{\mu_t}{\sigma_\varepsilon}\right)\frac{\partial \varepsilon}{\partial x_i}\right] + C_{1\varepsilon}\frac{\varepsilon}{k}(G_k + C_{3\varepsilon}G_b) - C_{2\varepsilon}\rho\frac{\varepsilon^2}{k} \qquad (9)$$

In these equations, G_k represents the generation of turbulent kinetic energy due to the mean velocity gradients. G_b is the generation of turbulent kinetic energy due to buoyancy. Y_M represents the contribution of the fluctuating dilatation in compressible turbulence to the overall dissipation rate. $C_{1\varepsilon}$, $C_{2\varepsilon}$ and $C_{3\varepsilon}$ are constants. σ_k and σ_ε are

the turbulent Prandtl numbers for k and ε, respectively.

The "eddy" or turbulent viscosity, μ_t, is computed by combining k and ε as follows:

$$\mu_t = \rho C_\mu \frac{k^2}{\varepsilon} \tag{10}$$

where C_μ is a constant.

The model constants $C_{1\varepsilon}$, $C_{2\varepsilon}$, C_μ, σ_k, and σ_ε have the following default values [11]:

$C_{1\varepsilon} = 1.44$ $\sigma_k = 1.0$

$C_{2\varepsilon} = 1.92$ $\sigma_\varepsilon = 1.3$

$C_\mu = 0.09$

The simulation was done using the standard $k-\varepsilon$ model. The general purpose CFD package PHOENICS is used to solve the governing equations. The model was run until a final converged solution was obtained by comparing the mass balances from the result file generated during the simulation. The model gives the two-dimensional plots for the velocity vectors, velocity contours, turbulence characteristics and pressure drop in the vessel.

4. RESULTS

Figure 2 (a) illustrates the velocity field for flow in the unpacked vessel. The results indicate that the jets hit the opposite wall of the converter with a high velocity and subsequently move towards the outlet. Despite a high injection velocity of 57 m/s, there are many zones inside the converter where the velocities are very small. These zones are referred to as zones with low velocities and sometimes as 'dead' zones. The ultimate objective is to reduce the size of such zones and to increase the velocity in these zones. These zones are observed between the jets and next to the vertical walls.

Figures 2 (b) and Figure 2 (c) illustrates the contours of the velocity in the y- and z-directions respectively. These velocities are referred to as V1 and W1 in all the following numerical results. When the flow is mainly unidirectional, these contour plots of V1 and W1 could be very useful. Figure 2 (b) highlights the abovementioned zones of low velocity.

Figure 3 (a) illustrates a plot of the y-directed velocity in the vessel at a distance of 2.5 m from the vessel bottom, or at a slab where z corresponds to the 25th row of cells, and Figure 3 (b) is a similar plot of the z-directed velocity. These values have been monitored at a central slab (z=25) which is seen to be the area of largest low velocity. The three peaks in Figure 3 (b) represent the three incoming jets. The zones of low velocity can be seen in the plots as a major part of the area between two consecutive jets. One way to quantify the extent of dead zoning or low velocity zones from these plots is by drawing two horizontal lines on these plots at +5 m/s and -5 m/s.

The variation in case of Figure 3 (a) (V1 velocities) shows that the velocities in most of the cells lie in the +5 to - 5 m/s range.

It can be seen from Figure 3 (b), that in between the first two jets there are 7 cells, whereas in between the second and third jet, there are 11 cells. The more the number of cells, the wider the low velocity zones.

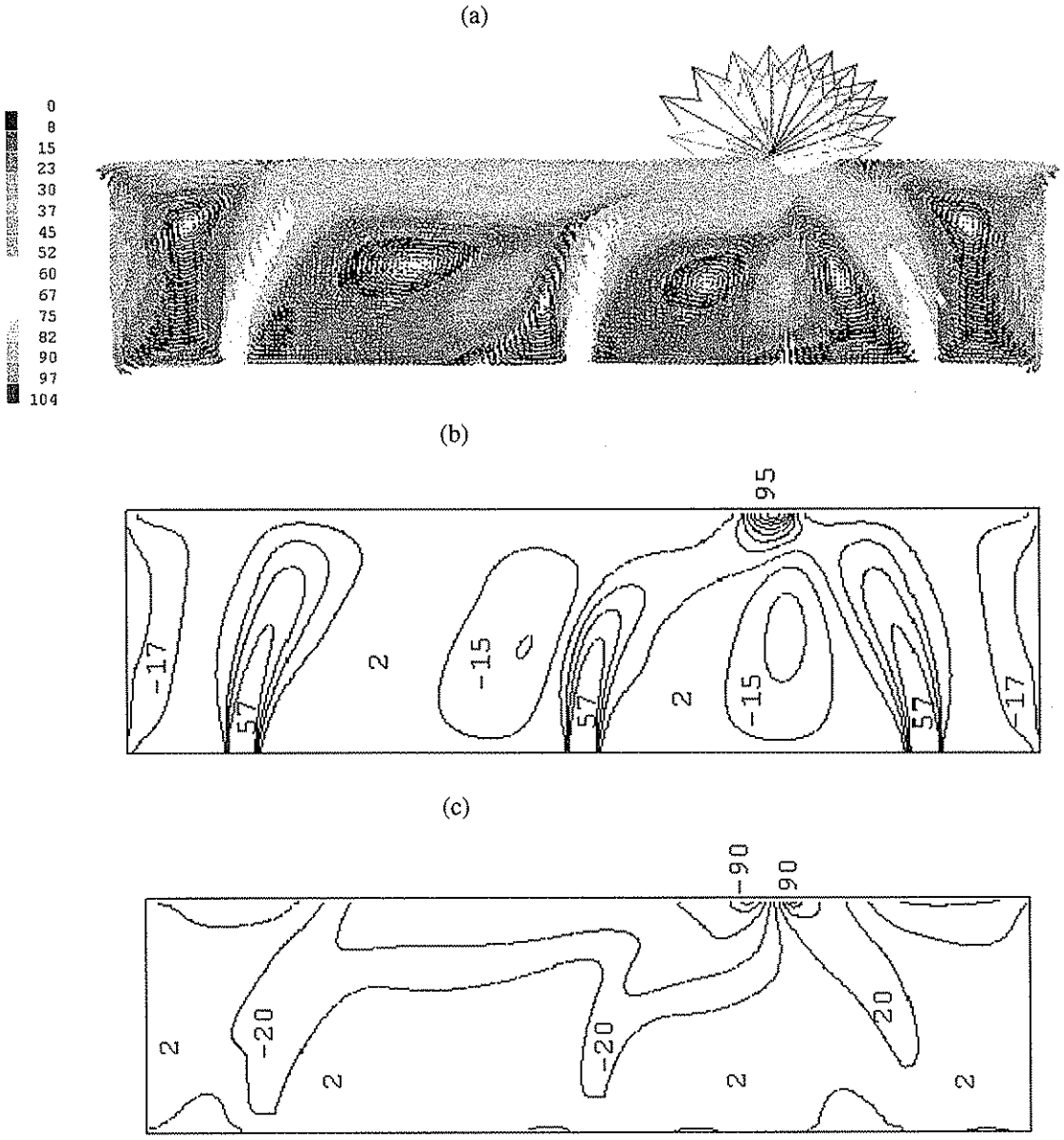

Figure 2 (a) Velocity Field for 57 m/s, (b) Contours of the velocity in the z- direction (W1) and (c) Contours of the velocity in the y-direction (V1)

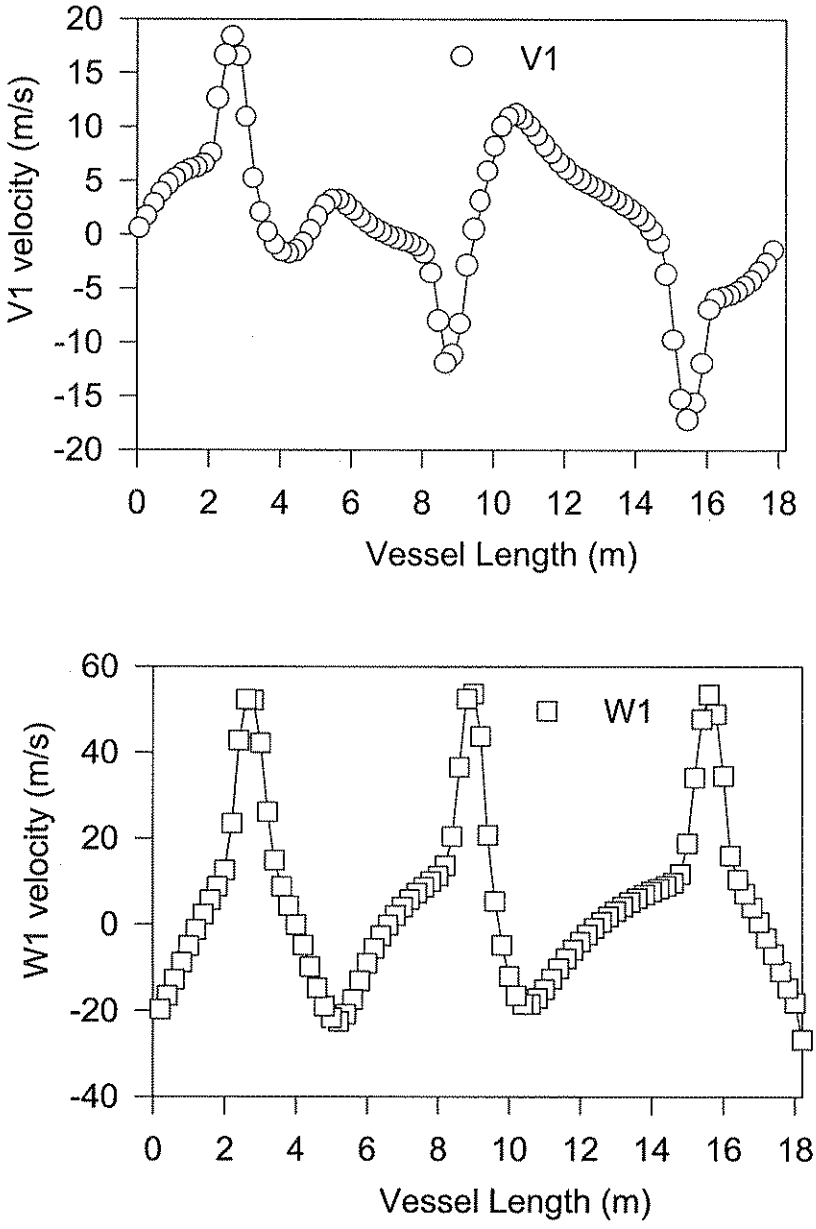

Figure 3. A plot of the (top) V1 velocity across the vessel at slab 25, and (bottom) W1 velocity across the vessel length at slab 25

4.1. Effects of the Fluid Flow Rate

The injection velocity was increased keeping the area of the inlets constant. Results show no appreciable improvement in the flow distribution as the injection velocity is increased by 55.6%, i.e., from 45 m/s to 57 and 70 m/s. Figure 4 illustrates this comparison of W1 for slab 25 (corresponding to the 25th row of cells) for the three cases. A comparison of V1 for these three cases shows similar trend to that of W1, i.e. no significant reduction in the size of the low velocity zones.

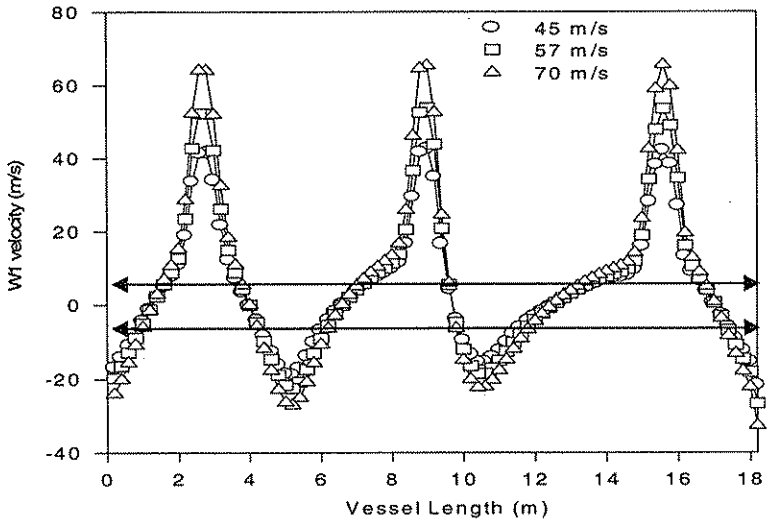

Figure 4. A plot of W1 versus the vessel length for slab 25 at three different injection velocities

4.2. Effects of Different Arrangements of Inlets & Outlets

Figure 5 illustrates a comparison of the W1 velocities flow field for three selected arrangements keeping the same inlets and varying the number of outlets. When the number of outlets is changed, the total area of all outlets is kept constant. The size of the zones with low velocity is smaller in the case of two-outlets compared to that of one outlet. It can also be seen that these low velocity zones are the smallest for the case with a multiple outlet.

A comparison of V1 velocities is not shown here, but it shows a similar trend to W1, that is a better flow distribution is obtained when two or multiple outlets are used instead of one.

Figures 6 shows a comparison of V1 velocity for three cases: the first one is 6 inlets and one outlet, the second is eight inlets and one outlet and the third case is multiple (sparged) inlets and multiple outlets. It can be stated that all the three arrangements of inlets and outlets did not give a much superior flow distribution and did not succeed in eliminating the zones of low velocities. The total size of these low velocity zones may change from case to case, however the flow distribution in 6-inlets/ 1 outlet and 8-inlets/ 1 outlets does not form a major step change from the standard case. These arrangements were chosen to investigate the effects of re-circulation flow but no great difference was observed. The multiple inlets/multiple outlets gave the best flow distribution as expected.

4.3 Effects of Internal Geometric Improvements

As a possible way of improving the flow distribution inside the unpacked vessel, an annular disc is inserted above each incoming jet in the original vessel geometry. Various inserts have been tried. In one case three discs are inserted, one above each incoming jet. Each disc has an inner (open) diameter of 0.4 m and an outer

diameter of 1.6 m. These discs are placed 0.6 m above the incoming jets. This resulted in significantly higher velocities at the bottom section of the vessel. However no

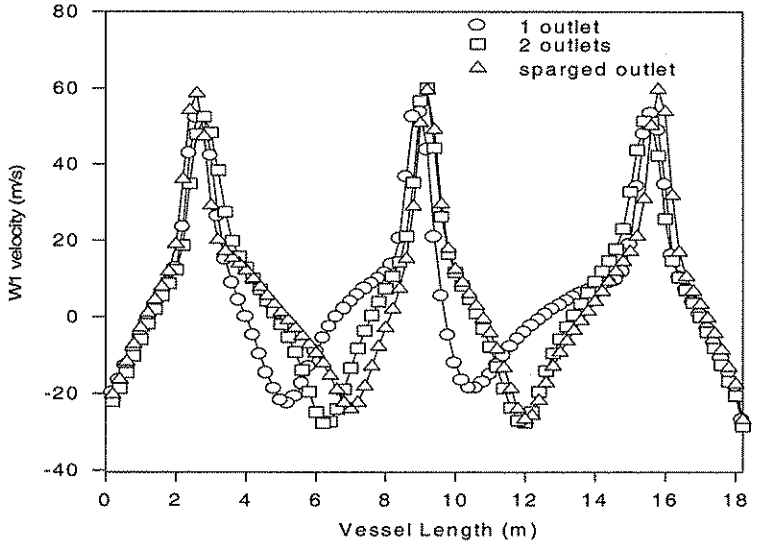

Figure 5. A plot of W1 versus the vessel length for slab 25 at three different outlet arrangements.

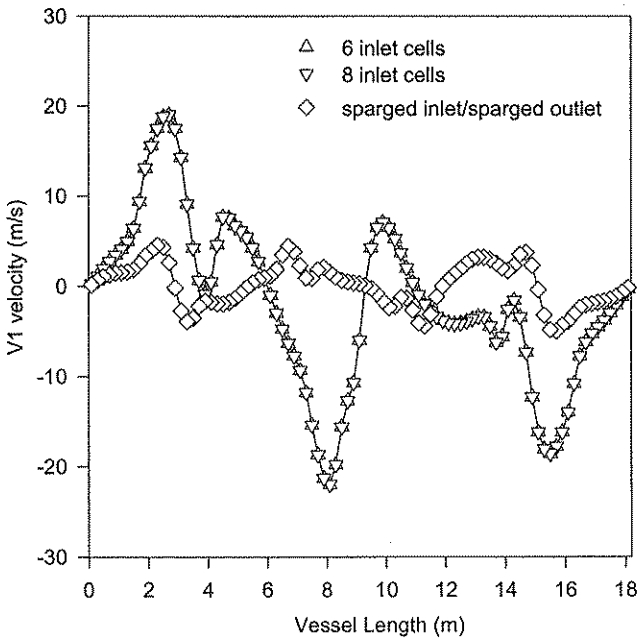

Figure 6. A plot of V1 versus the vessel length for slab 25 for three different inlet/outlet arrangements.

significant change was observed in the sizes of the zones with low velocities around the middle of the vessel. In another case similar discs but now with an open diameter of 0.2

m and an outer diameter of 1.0 m. Results show remarkable improvements in the flow patterns as compared to the previous case.

Another feasible option, which may be investigated, is to vary the shape and size of the inserts. Figure 7 (a), (b) illustrates the velocity field, and W1 contours respectively for the case with conical inserts, which can throttle the flow gradually and uniformly. The insert has 0.2 m diameter at the base which is gradually increased to 1.4 m at the top. This insert is placed at a distance of 0.4 m from the vessel bottom. Although the low velocity zones do not seem to have reduced, there is a good potential for a similar insert to split and guide the flow in order to minimize the size of the low velocity zones. It should be noted that all the three jets unite near the outlet with a high velocity. This arrangement may lead to a substantial elimination of low velocity zones in the vessel, because the discs provide a bi-directional jet, which maintains high activity to its left as well as to its right. There is a need to modify this insert, possibly to revert to a wider open base, say 0.4 m instead to 0.2 m and to narrow the cone angle. For this geometry, it is clear from Figure 7 (a), that across the middle z-plane , the low velocity zones has been significantly reduced. However larger low velocity zones are now observed in upper or lower parts of the vessel.

4.4. Effects of Turbulence Model

The base case (3 inlets, 1 outlet, no inserts) has also been simulated using the Reynolds Stress Turbulence Model (RSM) instead of the $k-\varepsilon$ model. The RSM is likely to provide a more realistic and rigorous approach for complex engineering flows. In this investigation, there seems to be some differences in the flow fields when RSM is used instead of the standard $k-\varepsilon$ model. The low velocity zones which were visible with the $k-\varepsilon$ model near the walls have been reduced to some extent. Results with RSM show higher recirculation than the $k-\varepsilon$ model leading to a better flow distribution near the walls. Although the RSM model has improved the flow situation to some extent, the computation time was almost 50% more than that with the $k-\varepsilon$ model. Thus the choice of the $k-\varepsilon$ model for this investigation is justified, considering the saving in computation time and accuracy in predicting the flow distribution in the vessel.

4.5. Simulation results with modified Ergun equation

All the results presented so far are for an unpacked vessel. In this section results for a partially packed vessel are presented. The vessel simulated here has the same dimensions as before except that a packed column 1.2 m high is placed 1.4 m above the vessel bottom. This means that cells located between 15-26 signify the bed. The modified Ergun equation was used in resolving the flow in the packed bed. The pressure force terms F_z and F_y for the packed bed are calculated from correlations (Equations 1-4). The bed is assumed to have a voidage of 0.5. The particle considered here are spheres of average diameter of $1/8^{th}$ of an inch. Figure 8 (a) show the result with $F_z = 10$ and $F_y = 10$ for the packed bed. The zone near the first two inlets has more activity as far as flow distribution is concerned as compared to that near the third inlet.

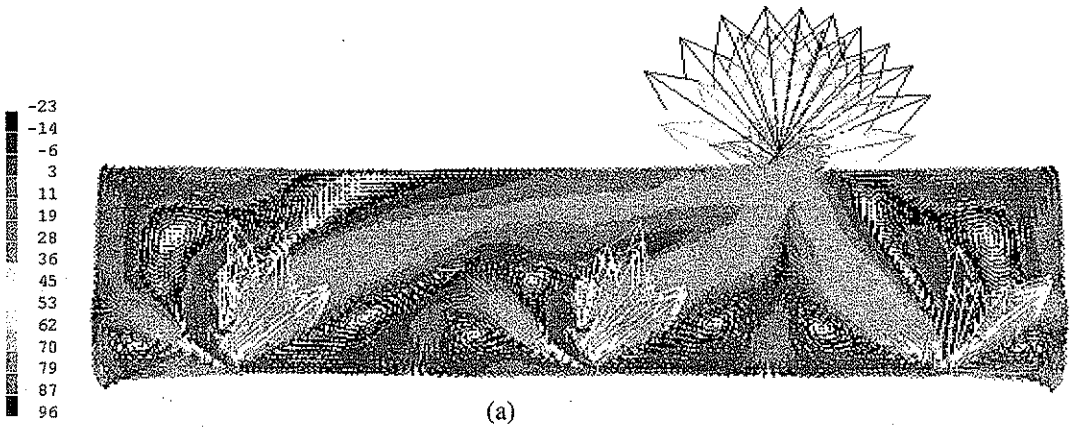

(a)

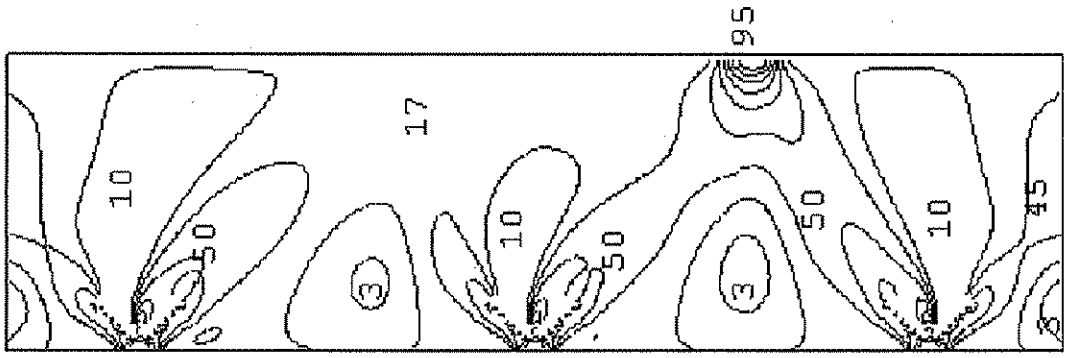

(b)

Figure 7. Annular Disc 0.2 m ID 1. m OD. (a) Velocity field at 57 m/s, and (b) Contour of the velocity in the z- direction (W1).

The effect of varying the values of F_z and F_y have been examined. Figure 8(b) shows the contours of the W1 velocity for $F_z = 100$, and $F_y = 10$. The results shown in this case are similar to those of $F_z = 10$. Here the second jet has broken contact with the first one. Figure 8(c) shows the contours of the W1 velocity for a case with $F_z = 5000$, $F_y = 5000$. The results shown in Figure 8(c) depict an almost uniform z-velocity distribution in the vessel. This result is very much similar to that obtained with the Darcy law model with permeability of $2.44e^{-8}$ (plot not shown here). The results indicate that at this high value of friction resistances, the bed acts as a uniform flow distributor. Figure 9 shows plots for z- directed velocity in slabs 15-22. The results show higher velocities in the bed at the 15^{th} cell (bed entrance), but once the fluid enters the bed, the velocity starts to fall and eventually at the 22^{nd} cell, which is somewhere near the bed center, the velocity throughout the bed is almost constant at about 5.6 m/s.

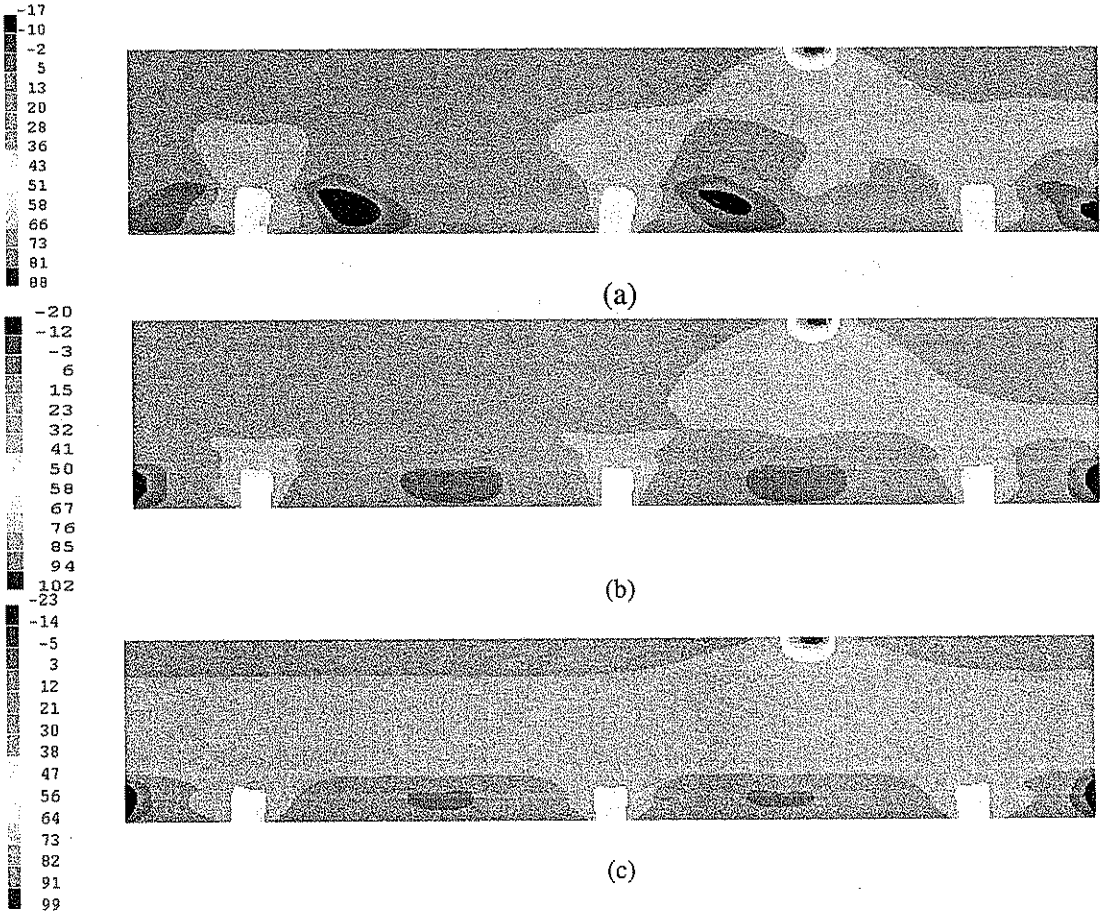

Figure 8. Contours of W1 for the packed bed, (a) (F_z = 10 and F_y = 10), (b) (F_z=100, F_y=10) , (c)(F_z =5000, F_y = 5000).

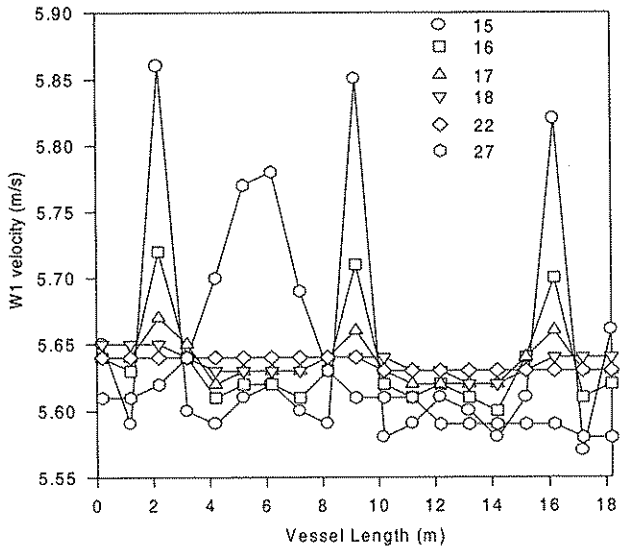

Figure 9. A plot of velocity in the z- direction for the packed bed with F_z = 5000 and F_y = 5000 at various positions in the bed

5. CONCLUSIONS

The present study showed that the flow distribution is significantly uneven in an unpacked vessel with three inlets and one outlet. A number of low velocity zones are observed. An increase of about 60% in the fluid flow rate has no pronounced effect on the flow situation in the vessel. The arrangements of inlets and outlets have a reasonable impact on the flow distribution in the unpacked vessel. The multiple inlets/multiple outlets case yields the best results as far as inlet/outlet modifications are concerned.

The flow distribution can also be enhanced by inserting some form of disc or flow redistributors in the vessel. The results with a 0.2 m insert as well as that with a conical insert give the best results. The results show that the conical insert can act as a good flow distributor in the vessel and if properly selected could lead to substantial improvements in the flow distribution.

For the partially packed case, the packed beds acted a good distributor of the flow, however, some limited maldistribution of flow was still observed. It is expected that such unevenness in the flow may be more pronounced in a three-dimensional case. This makes three dimensional model necessary. Work is being done in this regard.

The results with the modified Ergun approach are also interesting. The friction factor values that have calculated form these equations were very high. The results with a high value of the friction factor shows an almost constant flow in the bed. This result is much similar to the Darcy model results for the higher permeability. When the friction factors were reduced to a much lower value, the results show similar short-circuiting of flow pattern as with the Darcy model with a lower permeability.

Acknowledgement-The authors are grateful for the support of King Fahd University of Petroleum & Minerals during the course of this work and the preparation of this paper.

6. REFERENCES

1. R. V. A. Oleimans, *Computational Fluid Dynamics for the Petrochemical Process Industry*, Kluwer Academic Press, Netherlands, 1991.
2. D. A. Coleman, Computational Fluid Dynamics: Understanding Unit Operations, BP Amoco Chemicals, *PTQ*, 1999.
3. R. Berninger, and D. Vortemeyer, Der Einflub von Versperrung auf das reaktionstechnische Verhalten eines adiabaten Festbettreaktors, *Chemical Ingineer Technology*, **60**, 1052-1061, 1987.
4. J. Szekely, and J. J. Poveromo, Flow Maldistribution in Packed Beds, *Journal of The American Institute of Chemicl Engineers*, **21**, 769-781, 1975.
5. Y. Jiang, M. R. Khadilkar, M. H. Al-Dahhan and M. P. Dudukovic, Single Phase Flow Distribution in Packed Beds: Discrete Cell Approach Revisited, *Chemical Engineering Science*, **55**, 1829-1844, 2000.
6. I. Ziolkowska and D. Ziolkowski, Modeling of Gas Interstitial Velocity Radial Distribution over a Cross-Section of a Tube Packed with a Granular Catalyst Bed, *Chemical Engineering Science*, **48**(18), 3283-3292, 1993.
7. O. Bey, and G. Eigenberger, Fluid Flow Through Catalyst Filled Tubes, *Chemical Engineering Science*, **52**(8), 1365-1376, 1997.

8. D. Vortemeyer, and J. Schuster, Evaluation of Steady Flow Profiles in Rectangular and Circular Packed Beds by a Variational Method, *Chemical Engineering Science*, **38**(10), 1691-1699, 1983.
9. S. Ergun, Fluid Flow Through Packed Columns, *Chemical Engineering Progress, 48*(2), 89-94, 1952.
10. H. C. Brinkman, Fluid Flow in a Porous Medium. *Applied Science research Section. A1*, **27**, 143-149, 1947.
11. The PHOENICS Manuals, CHAM, London, UK, 1999.